Mutations in Yeast Calmodulin Cause Defects in Spindle Pole Body Functions and Nuclear Integrity

Ge-Hong Sun, Aiko Hirata,* Yoshikazu Ohya, and Yasuhiro Anraku

Department of Biology, Faculty of Science, and *Institute of Applied Microbiology, University of Tokyo, Hongo, Bunkyo-ku, Tokyo 113, Japan

Abstract. Yeast calmodulin (CaM) is required for the progression of nuclear division (Ohya, Y. and Y. Anraku. 1989. *Curr. Genet.* 15:113–120), although the precise mechanism and physiological role of CaM in this process are unclear. In this paper we have characterized the phenotype caused by a temperature-sensitive lethal mutation (*cmdl-101*) in the yeast CaM. The *cmdl-101* mutation expresses a carboxyl-terminal half of the yeast CaM (Met^{72}-Cys^{147}) under the control of an inducible *GAL1* promoter. Incubation of the *cmdl-101* cells at a nonpermissive temperature causes a severe defect in chromosome segregation. The rate of chromosome loss in the *cmdl-101* mutant is higher than wild-type cell even at permissive temperature. The primary visible defect observed by immunofluorescence and electron microscopic analyses is that the organization of spindle microtubules is abnormal in the *cmdl-101* cells grown at nonpermissive temperature. Majority of budded cells arrested at the high temperature contain only one spindle pole body (SPB), which forms monopolar spindle, whereas the budded cells of the same strain incubated at permissive temperature all contain two SPBs. Using the freeze-substituted fixation method, we found that the integrity of the nuclear morphology of the *cmdl-101* mutant cell is significantly disturbed. The nucleus in wild-type cells is round with smooth contours of nuclear envelope. However, the nuclear envelope in the mutant cells appears to be very flexible and forms irregular projections and invaginations that are never seen in wild-type cells. The deformation of the nuclear becomes much more severe as the incubation at nonpermissive temperature continues. The single SPB frequently localizes on the projections or the invaginations of the nuclear envelope. These observations suggest that CaM is required for the functions of SPB and spindle, and the integrity of nucleus.

CALMODULIN (CaM),[1] a ubiquitous eukaryotic Ca^{2+}-binding protein, mediates various Ca^{2+} signaling pathways (see review, Cohen and Klee, 1988). The Ca^{2+}/CaM complex is known to activate over 20 different enzymes including phosphodiesterase, brain adenylate cyclase, protein kinases, protein phosphatases and Ca^{2+}-ATPase. In addition, CaM has been shown to interact with many cytoskeletal components including MAP2 (microtubule-associated protein 2), tau, tubulin, and intermediate filament proteins (Cohen and Klee, 1988).

CaM has also been demonstrated to be an important component required for cell proliferation (see review, Anraku et al., 1991). In mammalian cells, an increase in the level of CaM accelerates the rate of cell proliferation (Rasmussen and Means, 1987), and a decrease in CaM induced by expression of its antisense RNA transiently arrests cell cycle progression in G1 and M phases (Rasmussen and Means, 1989). Deletion of the CaM gene (*CMD1*) in *Saccharomyces cerevisiae* (Davis et al., 1986), in *Schizosaccharomyces pombe* (Takeda and Yamamoto, 1987), or in *Aspergillus nidulans* (Rasmussen et al., 1990) causes a lethal phenotype. Phenotypic analysis of a conditional CaM-depleted mutant of budding yeast revealed that CaM is required for the progression of nuclear division and the fidelity of chromosome segregation (Ohya and Anraku, 1989*a*).

Several studies examining the indirect immunofluorescence localization of CaM in various cell types indicate that CaM is highly concentrated on the mitotic spindle apparatus of dividing cells (Welsh et al., 1978, 1979). Several CaM-binding proteins are also located in the mitotic spindle (Margolis et al., 1986, Brady et al., 1986). Microinjection of CaM into PtK_1 cells transiently protects kinetochore microtubules from the effect of nocodazole that disassembles the microtubules (Sweet et al., 1988). Together, these observations suggest that CaM may be an essential component of the mitotic apparatus. However, the molecular mechanism of CaM in regulating the function of mitotic spindle is still a matter of conjecture.

To understand the physiological significance of CaM in the mitotic process, we have undertaken genetic and cytological approaches to this issue using the yeast *S. cerevisiae*. This

1. *Abbreviations used in this paper*: CaM, calmodulin; DAPI, 4′,6-diamidino-2-phenylindole; SPB, spindle pole body; YP, 1% yeast extract, 2% polypeptone; YPD, YP supplemented with 5% glucose; YPGS, YP supplemented with 5% galactose, 0.2% sucrose.

eukaryotic microorganism is well suited for this endeavor, first because it possesses CaM with properties physiologically similar to those of higher organisms (Ohya and Anraku, 1989*b*, Davis and Thorner, 1989). Second, the yeast mitotic apparatus has been studied intensively by both cytological analysis and genetic dissection (Byers, 1981*a*, Winey and Byers, 1992).

Recently we have reported that the essential function of the yeast CaM in cell proliferation can be carried out by its derivatives, the half CaMs. Either the amino-terminal or carboxyl-terminal half of CaM complements the *cmd1* null mutation when they are expressed under a strong promoter, but not the authentic *CMD1* promoter (Sun et al., 1991). Cells depending solely on these half CaMs all show a temperature-sensitive phenotype for growth. This temperature-sensitive growth is rescued specifically by addition of 50 mM $CaCl_2$ to the medium (Sun et al., 1991).

In this paper, we describe the characterization of a temperature sensitive *cmd1-101* mutant expressing the carboxyl-terminal half CaM (Met^{72}-Cys^{147}). The *cmd1-101* mutant showed a severe defect in chromosome segregation. Immunofluorescence and electron microscopic analyses have revealed that the half CaM mutation affected the spindle organization, SPB functions and nuclear morphology.

Materials and Methods

Stains and Microbial Techniques

Yeast strains used in this work are listed in Table I. Yeast media and general genetic manipulations were carried out essentially as described in Rose et al. (1990). Yeast cultures were grown in YP (1% yeast extract [Difco Laboratories Inc., Detroit, MI], 2% polypeptone [Nihon Seiyaku, Tokyo, Japan]) supplemented with 5% glucose (YPD) or with 5% galactose and 0.2% sucrose (YPGS). YPD and YPGS supplemented with 100 mM $CaCl_2$ were used as Ca^{2+}-rich media. Synthetic minimal media (SD and SGS) supplemented with appropriate nutrients were used to select for plasmid maintenance and gene replacement. All yeast transformations were carried out by the lithium acetate method of Ito et al. (1983).

For construction of the strain carrying the *GAL1-cmd1-101* fusion gene integrated at the chromosomal *CMD1* locus, the plasmid pGCAMTC1 for integration was constructed as follows. The 0.8-kb *HincII-StuI* fragment of *TRP1* gene from TRP/SK^+ (Sun et al., 1991) was inserted into the *StuI* site of pRSGCAMC1 (Sun et al., 1991) that carries the fusion gene of *GAL1p-cmd1-101*, creating plasmid pRSCAMCT1. A *Bam*HI linker (pCGGATCCG) was inserted into the *Sma*I gap on pRSCAMCT1, creating plasmid pRSCAMCBT1. The 1.4-kb *BglII-BglII* fragment carrying the *CMD1* gene on plasmid pCAM106 (Sun et al., 1991) was replaced by the 2.4-kb *Bam*HI fragment from pRSCAMCBT1, creating pGCAMTC1. The integration of *GAL1p-cmd1-101* fusion gene was performed by single step replacement (Rothstein, 1983). The *CMD1* parents of YPH499 and YPH500 were transformed with 2 μg of pGCAMTC1 linearized with *Bam*HI. Trp^+ prototrophs were selected and the allele replacement was confirmed by Southern analysis (Southern, 1975) using the 1.1-kb *BglII* fragment of the *CMD1* gene as a probe (data not shown).

For construction of strains bearing a marker chromosome for chromosome segregation assay, plasmid p300-1KMC was constructed by inserting the 1.5-kb *Bam*HI fragment of the *CMK1* gene, which is located on chromosome VI (Ohya et al., 1991), into the *Bam*HI gap of plasmid YCF4 (Vollrath et al., 1988) which contains the *SUP11*, *CEN4*, and *URA3*. Haploid strains GHGC1500 (*cmd1-101*) and YPH500 (*CMD1*) were transformed with 3 μg of p300-1KMC linearized with *BglII* and *Eco*RI. Transformants were selected on SGS (-uracil) plates. The presence of the marker chromosome was confirmed by OFAGE as described previously (Carle and Olson, 1984, 1985). The resulting strains from GHGC1500 and YPH500 are designated as GHGC300 and GHW300, respectively.

Bacterial strains DH5α (Bethesda Research Laboratories Inc., Gaithersburg, MD) and SCS1 (Stratagene Corp., San Diego, CA) were used for the propagation of plasmids. *Escherichia coli* cells were cultured in LB medium and transformed by the calcium chloride procedure as described previously (Maniatis et al., 1982).

Flow Cytometry

Yeast cells were prepared for flow cytometry essentially as described by Hutter and Eipel (1979) using propidium iodide (Sigma Chemical Co., St. Louis, MO). The culture of strain GHGC1501 (*cmd1-101/cmd1-101*) in early-exponential phase was shifted to 37°C. Cells (5×10^6) were collected, fixed in 70% ethanol and washed with 0.2 M Tris-Cl (pH 7.5) solution. The fixed cells were sonicated thoroughly, and treated with 1 mg/ml RNase A. Before analysis, the cells were stained with 5 μg/ml propidium iodide for 15 min on ice, and then analyzed on an Epics C system (Coulter Corp., Hialeah, FL).

Measurements of Chromosome Loss

Analysis of chromosome loss was performed using the chromosome fragment method as described by Shero et al. (1991). For color sectoring assay, strains GHGC300 and GHW300 were grown to early-exponential phase in SGS (-Ura) to prevent outgrowth of cells that had lost the marker chromosome. These cells were plated onto the YPGS solid medium, which is a condition allowing the loss of the marker chromosome. For quantitation of chromosome loss, the strains GHGC300 and GHW300 were first grown to early-exponential phase in the selective medium. These cells were then transferred to fresh YPGS medium and incubated for 4 h at 23°C or 30°C, or 3 h at 23°C and then 1 h at 37°C. Viability was determined by plating out a portion of the culture on YPGS plates. The remaining cells were collected from culture and plated on SGS plate containing 1 mg/ml 5-FOA (Sigma Chemical Co.) to select cells lacking a *URA3* chromosome fragment as described (Shero et al., 1991). The frequency of chromosome loss equals the number of Ura^- cells divided by the number of viable cells.

Immunofluorescence Microscopy

Immunofluorescent staining of yeast cells was performed using a method of Stearns and Botstein (1988) with modifications. Cells were fixed in 5% formaldehyde in YPGS for 30 min at room temperature. The cells were then collected and fixed in 3.7% formaldehyde in 0.1 M KPO_4, pH 7.5 for an additional 30 min. The fixed cells were spheroplasted in 0.1 M KPO_4, pH

Table I. Strain List

YPH499	*MATa ura3-53 lys2-80 ade2-101 trp1-Δ63 his3-Δ200 leu2-Δ1*	Sikorski and Hieter (1989)
YPH500	*MATα ura3-53 lys2-80 ade2-101 trp1-Δ63 his3-Δ200 leu2-Δ1*	Sikorski and Hieter (1989)
YPH501	*MATa ura3-53 lys2-80 ade2-101 trp1-Δ63 his3-Δ200 leu2-Δ1* *MATα ura3-53 lys2-80 ade2-101 trp1-Δ63 his3-Δ200 leu2-Δ1*	Sikorski and Hieter (1989)
GHGC1499	*MATa ura3-53 lys2-80 ade2-101 his3-Δ200 leu2-Δ1cmd1::GAL1p-cmd1-101-TRP1*	This study
GHGC1500	*MATα ura3-53 lys2-80 ade2-101 his3-Δ200 leu2-Δ1cmd1::GAL1p-cmd1-101-TRP1*	This study
GHGC1501	*MATa ura3-53 lys2-80 ade2-101 his3-Δ200 leu2-Δ1 cmd1::GAL1p-cmd1-101-TRP1* *MATα ura3-53 lys2-80 ade2-101 his3-Δ200 leu2-Δ1 cmd1::GAL1p-cmd1-101-TRP1*	This study
GHGC1502	*MATa ura3-53 lys2-80 ade2-101 his3-Δ200 leu2-Δ1 CMD1* *MATα ura3-53 lys2-80 ade2-101 his3-Δ200 leu2-Δ1 cmd1::GAL1p-cmd1-101-TRP1*	This study
GHGC300	*MATa lys2-80 ade2-101 his3-Δ200 leu2-Δ1 cmd1::GAL1p-cmd1-101-TRP1 SUP11:URA3*	This study
GHW300	*MATa lys2-80 ade2-101 trp1-Δ63 his3-Δ200 leu2-Δ1 SUP11::URA3*	This study

7.5, 1.2 M sorbitol. The spheroplasts were then applied to the wells of multiwell microscope slides (Flow Laboratories, Maclean, VA) precoated with 1% polylysine (Sigma Chemical Co.). Subsequent antibody incubation and washes were performed in PBS containing 1% BSA. The primary antibody used was YOL1/34 (Kilmartin et al., 1982), a rat mAb directed against α-tubulin (Sera-Lab, Sussex, England) diluted 1/50 (vol/vol). The secondary antibody was FITC-conjugated goat anti-rat IgG (Cappel Laboratories, Cochranville, PA) diluted 1/50 (vol/vol). All antibody dilutions were made in PBS containing 1% BSA and 0.1% sodium azide. Antibody incubations were performed for 1 h at room temperature. DNA was stained by a treatment with 1 μg/ml 4',6-diamidino-2-phenylindole (DAPI) for 1 min. Stained cells were examined with an Olympus BHS-FRCA epifluoresence microscope (Olympus Corp., Tokyo, Japan) and photographed on Kodak Ektachrome 400 film (Eastman Kodak Co., Rochester, New York).

Freeze-substituted Fixation Method of EM

Preparation of thin section of yeast cells by the freeze-substituted fixation method was carried out as described (Kanbe and Tanaka, 1989) with minor modifications. Diploid cells grown in YPGS medium at 23°C were shifted to 37°C. After incubation for a certain period, the cells were collected by centrifugation. Pellets of cells were mounted on the copper meshes to form a thin layer and plunged into liquid propane cooled with liquid N_2. Frozen cells were transferred to 2% OsO_4 in anhydrous acetone, kept at −80°C for 48 h in solid CO_2-acetone bath, then transferred to −35°C for 2 h, 4°C for 2 h, and to room temperature for 2 h. After washing with anhydrous acetone three times, samples were infiltrated with increasing concentrations of Spurr's resin in anhydrous acetone and finally with 100% Spurr's resin. These samples were then polymerized in capsules at 50°C for 5 h and 70°C for 30 h. Thin sections were cut on a Sorvall MT-2 ultramicrotome or Reichest Ultracut N, and then stained with uranyl acetate and lead citrate. Serial sections were viewed on a JEOL 200 CX electron microscope (JEOL USA, Inc., Peabody, MA) at 100 kV.

Three-dimensional Reconstitutions

Computer-aided reconstructions from images of serial thin sections were made using OSMOZONE 2AS (Nikon Inc., Tokyo). Briefly, prints of serial 100-nm sections were enlarged to a final magnification of 18,000 by xerographic copy. For each section, profiles of the nuclear envelope, the plasma membrane, and the microtubules were drawn on the sheets of xerographic copy. The sheets were then aligned by best fit of the profiles. These profiles were put into a computer (PC9801 Vm, NEC Co., Tokyo) using a digitizing tablet, and a profile-stack reconstruction was made. After the best viewing angle was established and shaded, solid-model views were made. The *x*- and *y*-axes of each three-dimensional reconstruction were equivalent to those obtainable by standard transmission electron microscopy, but in the *z*-axis it was limited to the section thickness (i.e., 100 nm). The three-dimensional image of type I cell was constructed based on 41 serial sections and that of type III cell was based on 29 serial sections that covering the entire nucleus.

Pulse-Labeling, Chase, and Immunoprecipitation

Cells were grown to 0.2 O.D.$_{600}$ (1 O.D.$_{600}$ unit = 1 × 10^7 cells) in synthetic minimal minus sulfate medium containing 100 μM $(NH_4)_2SO_4$. One O.D.$_{600}$ unit of cells was harvested, washed once with distilled water and resuspended in 720 μl of SGS minus sulfate medium. After incubation for 10 min at 30°C, 400 μCi Tran^{35}S label (ICN Biomedicals, Inc., Costa Mesa, CA) was added. The labeling time is 10 min. The chase was initiated with the addition of 80 μl of a solution containing 10 mM $(NH_4)_2SO_4$, 0.03% L-cysteine, and 0.04% of L-methionine and 650 μl of YPGS medium. Immediately after initiating the chase, equivalent aliquots (150 μl) of the suspension were transferred to fresh YPGS or YPGS plus 100 mM $CaCl_2$ media, and chased in the two media at either 30 or 37°C. Equivalent aliquots (1 ml) were removed at the indicated time point and added to equal volumes of ice-cold 20 mM sodium azide to terminate the chase. Labeled cells were washed with 1 ml of ice-cold 20 mM sodium azide, and resuspended in 200 μl of TBS containing 1% SDS, 1 mM PMSF, and 5 μg/ml each of leupeptin, antipain, pepstatin A, and chymostatin. Glass beads (200 mg) were added and the suspensions were vortexed at top speed for 2 min and then heated on a 100°C heat block for 5 min. Extracts were adjusted to a volume of 1 ml by addition of 2% Triton X-100 in TBS and clarified by centrifugation at 12,000 *g* for 15 min at 4°C. The supernatants were incubated with 1 μl IgG fraction of anticalmodulin polyclonal antibody (Ohya et al., 1987) on ice for at least 12 h and then with 20 μl of 50% (vol/vol) protein A-Sepharose CL-4B (suspension in TBS) with gentle agitation at room temperature for 2 h. The immunoprecipitates were collected by centrifugation and washed twice with 1 ml of 1% Triton X-100, 0.2% SDS, 150 mM NaCl, 5 mM EDTA, and 10 mM Tris-HCl, pH 8.0, twice with 1 ml of 2 M urea, 1% Triton X-100, 0.2% SDS, 150 mM NaCl, 5 mM EDTA, and 10 mM Tris-HCl, pH 8.0, once with 1 ml of 1% Triton X-100, 0.2% SDS, 500 mM NaCl, 5 mM EDTA, and 10 mM Tris-HCl, pH 8.0, and once with 1 ml of 150 mM NaCl, 5 mM EDTA, and 10 mM Tris-HCl, pH 8.0. The immunoprecipitates were eluted from the beads by heating at 100°C for 5 min in SDS gel sample buffer and subjected to SDS-PAGE as described (Laemmli, 1970). After electrophoresis, the gels were treated with Amplify (Amersham Corp., Arlington Heights, IL), dried and exposed to Kodak X-Omat AR film for 1–3 d at −80°C. The level of the CaM or half CaM was measured on a Shimazu Model CS-900 densitometer (Shimazu, Tokyo, Japan).

Results

Construction of the cmd1-101 Mutant

To characterize the phenotype of a mutant expressing the half CaM, the wild type *CMD1* genes of strains YPH499 (*MAT***a**) and YPH500 (*MATα*) were replaced with the fusion gene *GAL1*p-*cmd1-101* (Sun et al., 1991) expressing the half CaM (Met^{72}-Cys^{147}). The strategy for this gene replacement is schematically presented in Fig. 1. A 2.4-kb DNA fragment carrying the *GAL1*p-*cmd1-101* fusion gene and *TRP1* gene with 0.3 kb and 0.4 kb flanking the *CMD1* gene-replacing fragment was used to transform *trp1* haploid strains. Because depletion of the half CaM causes a lethal phenotype (Sun et al., 1991), cells carrying the integrated *cmd1-101* gene do not grow on medium containing glucose, where the *GAL1* promoter is switched off (Johnston and Davis, 1984). Therefore, we selected Glc$^-$ Trp$^+$ transformants. The correct fragment replacement at the *CMD1* locus was verified by Southern analysis using endonuclease digested DNA from seven individual transformants of each strain. In all the Glc$^-$ Trp$^+$ transformants the *CMD1* gene was replaced with the fusion gene (data not shown). The expressions of the half CaM from the strains carrying the fusion gene were confirmed by immunoprecipitation with antiyeast CaM antibody (see below). The diploid strain (GHGC1501) was obtained by mating GHGC1499 (*MAT***a**, *cmd1-101*) and GHGC1500 (*MATα*, *cmd1-101*), which were derived from YPH499 and YPH500, respectively.

We have examined whether the deletion of the region adjacent to the *CMD1* gene (see Fig. 1) had any effect on the phenotype of the *cmd1-101*. First, we transformed the *cmd1-101* cells with a plasmid pGCAM105 expressing the coding region of the native CaM under the *GAL1* promoter: pGCAM105 complemented completely the temperature sensitive defects observed in the *cmd1-101* mutant (data not

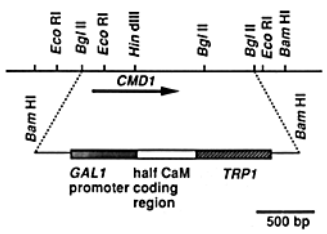

Figure 1. Scheme of the strategy for construction of the *cmd1-101* mutant. The 2.4 kb *Bam*HI fragment of pGCAMTC1 was used to transform haploid strains YPH499 (*MAT***a** *CMD1*) and YPH500 (*MATα* *CMD1*). The Glc$^-$Trp$^+$ transformants were picked and the integrations of the *GAL1*p-*cmd1-101* fusion gene into the chromosomal *CMD1* locus were verified by Southern analysis.

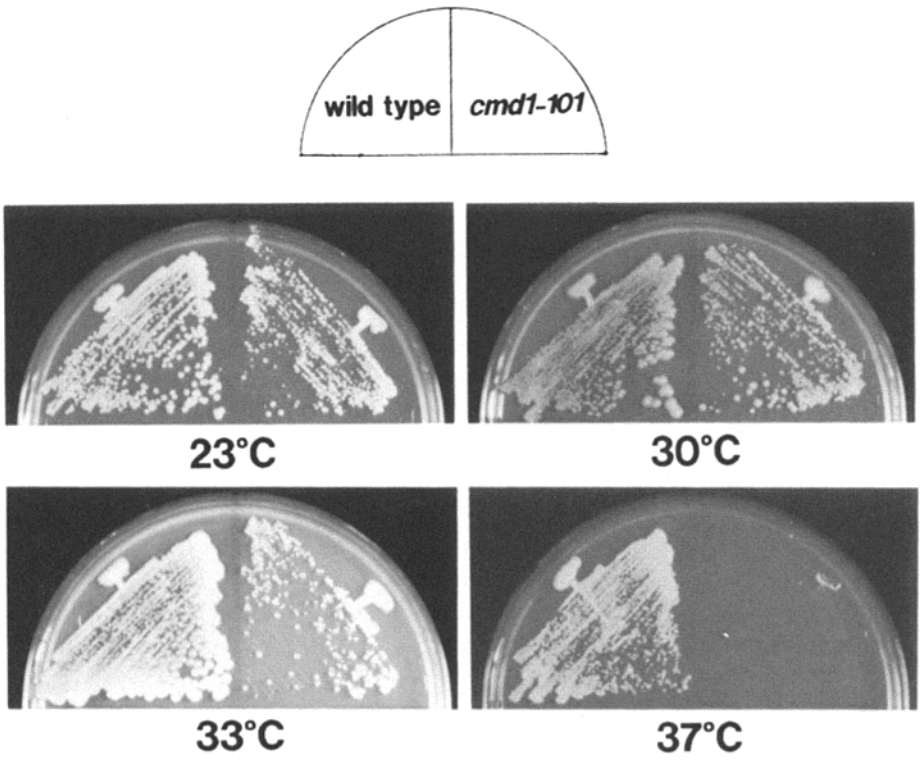

Figure 2. The Ts⁻ growth phenotype of the *cmdl-101* mutant cell. Cells isolated from a single colony of a *cmdl-101* diploid strain (GHGC1501) were streaked on YPGS plates. After incubation at 23, 30, 33, and 37°C for 4 d, the plates were photographed. The *cmdl-101* cells formed colonies at 23, 30, and 33°C, but did not grow at 37°C. A wild-type strain (YPH501) was used as the control.

shown). We have also examined another deletion construction (*cmdl-Δl*) which deletes 3/4 of the *CMD1* gene within its coding region (Sun et al., 1991). Cells containing *cmdl-Δl* and a centromere-based plasmid pRSGCAMC1 (Sun et al., 1991) expressing the half CaM under the *GAL1* promoter showed a temperature sensitive phenotype and aberrant microtubule organization (see below) similar to the *cmdl-101* mutant cells. These results confirmed that the phenotype exhibited in the *cmdl-101* mutant was due to the mutations in the *CMD1* gene.

The cmdl-101 Mutant Shows Defects in Mitosis at Nonpermissive Temperature

The *cmdl-101* cells were capable of growth at 23, 30, and 33°C on YPGS medium. However, the *cmdl-101* cells did not grow at 37°C (Fig. 2). Upon shift to 37°C, the *cmdl-101* cells (GHGC1501) stopped growth within 3 h (Fig. 3 *A*). Cell division ceased within two rounds, as judged by the number of cells in microcolonies formed from single cells on agar medium using time lapse photomicroscopy (Hartwell, 1971, 1978). The *cmdl-101* mutation is lethal at the restrictive temperature; cells transferred to 37°C for 4 h yield <10% viable cells when returned to the permissive temperature (23°C) (Fig. 3 *B*). Microscopic examination of the GHGC1501 (*cmdl-101/cmdl-101*) cells after the shift to 37°C for 4 h revealed that ~90% of cells appeared with buds; 80% containing large buds and 10% small buds (Fig. 4 *B*). DAPI staining of nuclear DNA showed that >98% of cells incubated at the nonpermissive temperature were arrested with a single nucleus (see below: Fig. 7 *C–E*).

In *S. cerevisiae*, cell morphologies are good measures for distinguishing the stage of cell cycle. However, this measure alone cannot determine a specific defect either in chromosome segregation or in DNA synthesis, because both defects cause growth arrest as mononucleated large budded cells. The point of accumulation in the cell cycle can be more precisely determined by flow cytometric analysis of DNA content of the arrested cells. Diploid cells (GHGC1501) grown in YPGS medium at 23°C generated two peaks, one corresponding to the fraction of cells in the population with 2c content of DNA, and the other to cells with 4c content of DNA (Fig. 5, *top*). Upon shift to 37°C, the proportion of 4c cells increased while that of 2c cells decreased. After incubation at 37°C for 5 h, almost all the cells were arrested with 4c DNA content (Fig. 5, *bottom*). The increased fluorescence at the later time points was due to the contribution of mitochondrial DNA to the fluorescent signal, because the

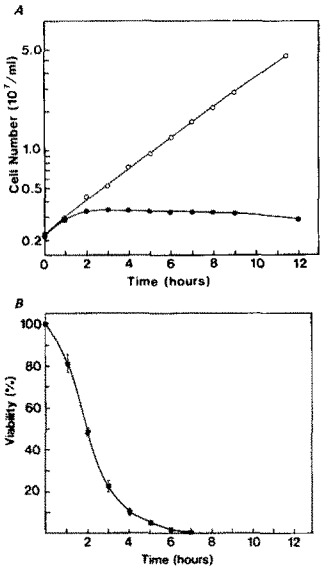

Figure 3. Temperature sensitive growth property of the *cmdl-101* mutant. (*A*) At zero time, diploid strain GHGC1501 (*cmdl-101/cmdl-101*) grown to early-exponential phase in YPGS medium at 23°C were divided into two parts, half of the culture continued to be incubated at 23°C (*open circles*), the other half were shifted to 37°C (*closed circles*). (*B*) Viability of the cells grown at nonpermissive temperature was determined by plating out a portion of the culture on YPGS plates and incubated at 23°C (*closed squares*).

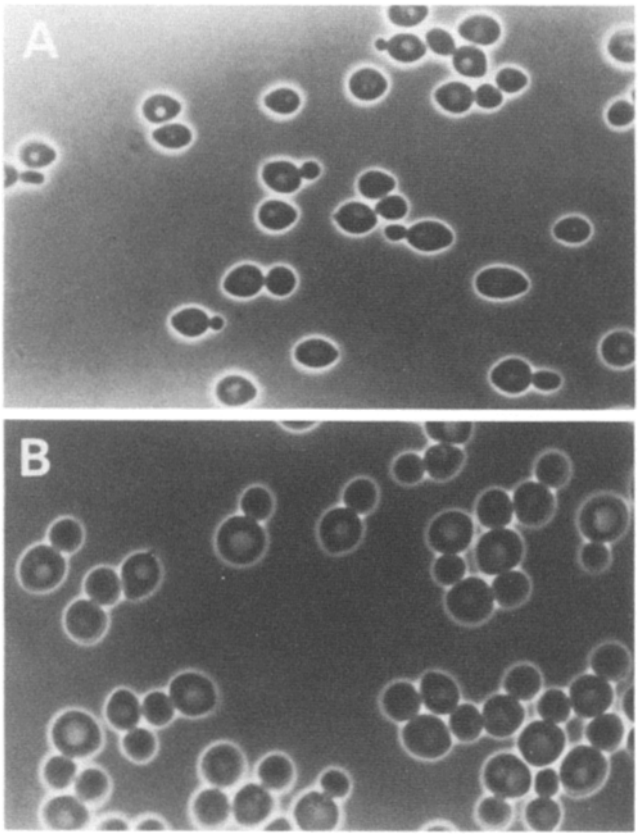

Figure 4. Cell cycle arrest morphology caused by the *cmdl-101* mutation. Exponential phase cultures of *cmdl-101* diploid strain (GHGC1501) in YPGS at 23°C were shifted to 37°C. (*A*) The morphology of the *cmdl-101* cells incubated in YPGS at 23°C; (*B*) the *cmdl-101* cells incubated in YPGS 4 h after shift to 37°C.

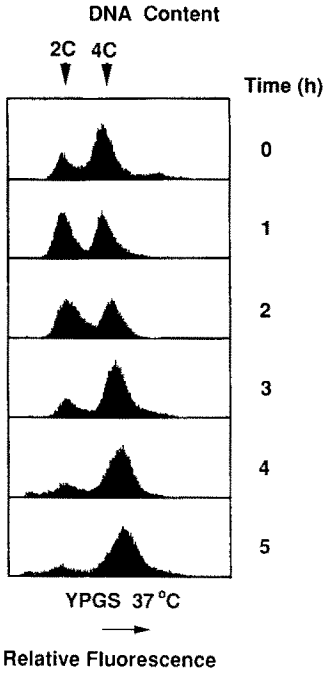

Figure 5. Flow cytometric analysis of the DNA contents of the *cmdl-101* cells grown in YPGS medium at 37°C. Cells of diploid strain GHGC1501 (*cmdl-101/cmdl-101*) grown to early-exponential phase in YPGS medium at 23°C were shifted to 37°C. Cells were withdrawn at intervals, fixed, stained with propidium iodide, and subjected to flow cytometric analysis. For each sample, 20,000 fluorescent events were measured. The *cmdl-101* mutant cells arrested with G2/M DNA content.

volume of the GHGC1501 cell arrested at the high temperature is increased nearly eight times (see Fig. 4 *B*, Nisogi et al., 1992, Daniel et al., 1991). The DNA content per cell was also confirmed by the VIMPCS (video-intensified microscope photon counting system; Kuroiwa et al., 1986) which measured the amount of nuclear DNA specifically (data not shown). Therefore, the *cmdl-101* cells were arrested at the G2/M phase without undergoing an additional S phase. Moreover, we found that the appearances of DAPI staining were not uniform. The DAPI blobs frequently appeared to be twisted or slightly stretched were not uniform. The DAPI blobs frequently appeared to be twisted or slightly stretched (Fig. 7 *C*), suggesting that the nuclear elongation occurred. These results indicate that the *cmdl-101* cells are arrested during the process of mitosis.

The cmdl-101 Mutant Has a Defect in Chromosome Segregation

The effects of the *cmdl-101* mutation on chromosome stability were examined using the colony color sectoring assay (Shero et al., 1991). Yeast cells with a nonsense mutation *ade2-101* in the *ADE2* gene accumulate a red pigment and thus turn red upon growth on solid medium. This red color is not detected when the cell contains a tRNA suppressor that can suppress the *ade2-101* nonsense mutation. The loss of the tRNA suppressor during colony development allows the accumulation of pigment in the resulting clonal lineage. A 10-kb plasmid p300-1KMC (*SUP11*, *CEN4*, and *URA3*) linearized with *Eco*RI and *Bgl*II was used to transform the *cmdl-101* mutant (GHGC1500) as well as its isogenic wild-type strain (YPH500). This manipulation generated a nonessential marker chromosome carrying the *CEN4*, *URA3*, *SUP11*, and a part of the chromosome VI. After growing cells containing the marker chromosome to exponential phase in selective medium, the cells were plated onto YPGS medium (see Materials and Methods). The sectoring patterns are shown in Fig. 6. A portion of colonies of the mutant cells were red or containing red sectors (Fig. 6 *B*), whereas wild-type colonies were almost all white (Fig. 6 *A*). This result clearly showed that the half CaM mutant cell lost the marker chromosome at a higher frequency than the wild-type cell did.

Next, we examined the rate of chromosomal loss by counting the colonies formed on plates containing 5-fluoro-orotic acid (5-FOA). This compound is converted to a toxic product, 5-fluorouracil, through the action of the decarboxylase, which is encoded by the *URA3* gene. Therefore, *ura3* cells are resistant to 5-FOA, whereas *URA3* cells are killed on the 5-FOA plate. This method is used to select cells lacking the marker chromosome fragment carrying the *URA3* gene (Boeke et al., 1987; Shero et al., 1991). The strains containing the marker chromosome were first grown to early-exponential phase in selective medium at 23°C and then transformed to fresh YPGS medium for 4 h at different temperatures before plating onto 5-FOA plates. The *cmdl-101* mutant showed an increased frequency of chromosome loss after being incubated at the nonpermissive temperature for 1 h (Table II). In addition, the half CaM mutant had a 50-fold higher rate of chromosome loss compared to the wild-type strains even at the permissive temperature. These results indicate that the half CaM mutant has a defect in accurate chromosome segregation.

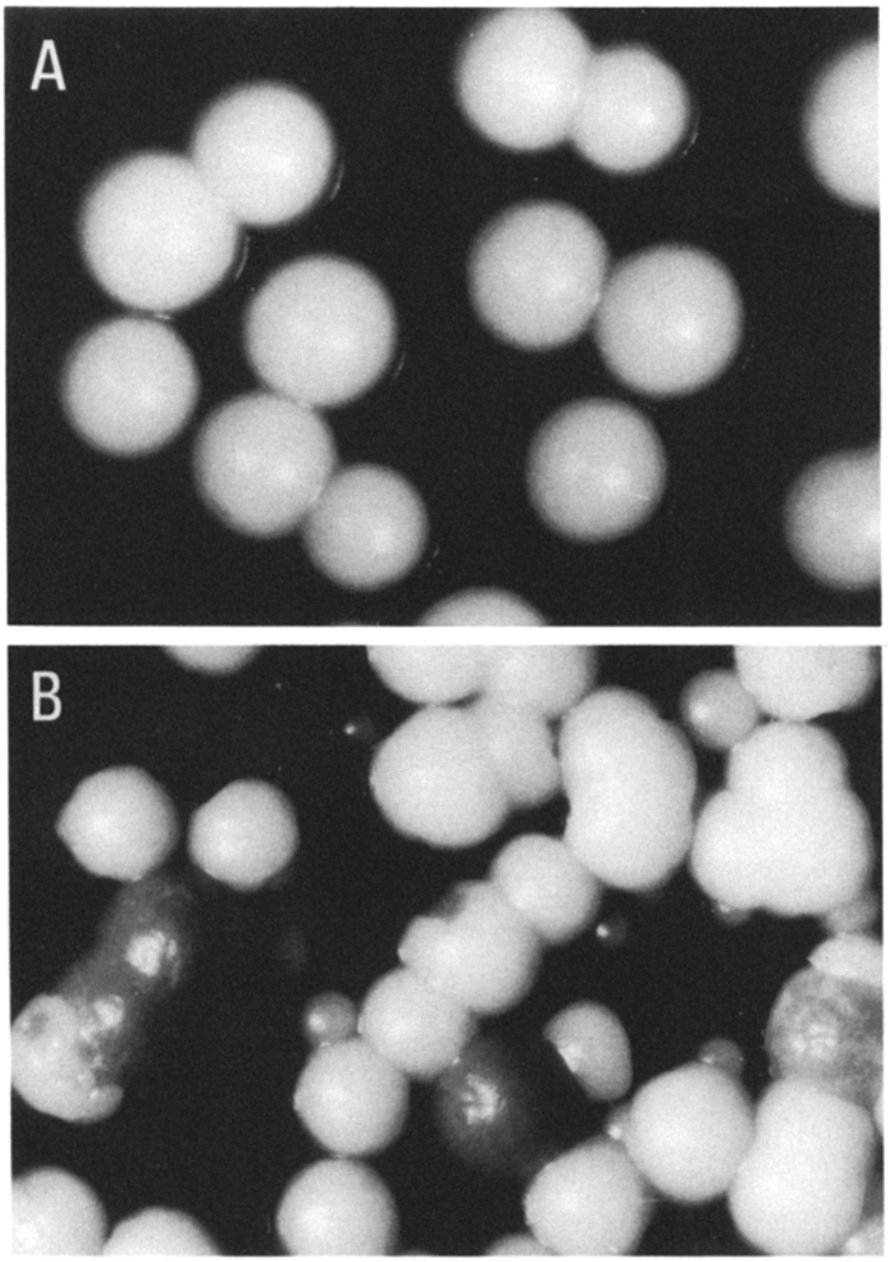

Figure 6. The half CaM mutant cells lose the artificial marker chromosome faster than the wild-type cells. GHW300 (wild-type) and GHGC300 (*cmdl-101*) were grown in uracil-free medium to early-exponential phase. The cells were diluted with sterile water and plated on YPGS plates to form sectors. Cells were allowed to grow at 23°C for at least 48 h and placed at 4°C for 48 h to help color development. (*A*) GHW-300 cells. Colonies were all white. (*B*) GHGC300 cell. A portion of colonies were red or contained red sectors.

The Strain Containing cmdl-101 Produces a Monopolar Spindle

The stage of the cell cycle at which the *cmdl-101* mutant cells were arrested was examined in more detail by examining the microtubule organization in the *cmdl-101* diploid strain incubated at 37°C by immunofluorescence microscopy. As seen in Fig. 7 *A*, the microtubules in wild-type cells were found to be associated exclusively with the SPB(s) and the cytoplasmic microtubules were not prominent. The staining patterns of microtubules in the *cmdl-101* cells grown in YPGS medium at 23°C (Fig. 7 *B*) were almost indistinguishable from that seen in wild-type cells (Fig. 7 *A*). However, the microtubule organization observed in the *cmdl-101* cells incubated at the nonpermissive temperature was apparently disturbed. Fig. 7, *C–E*, show three typical staining patterns of microtubules observed in the large-budded cells of the *cmdl-101* mutant 3 h after transfer to 37°C. In the first class (type I), the mutant cells contained one focus of microtubules that was associated with the nuclear DNA (Fig. 7 *C*). The second form (type II) is the cells containing one cluster of microtubules that was not associated with the nuclear DNA (Fig. 7 *D*). Both type I and type II cells apparently did not exhibit any spindlelike structures. The third type is the cells containing a very short spindle or a microtubule organization that appeared like a short spindle (Fig. 7 *E*). The distribution and temporal relationship of the three staining patterns in the population are shown in Fig. 8. We found that only a small fraction of the cells exhibited short spindle (or type III) morphology, and fewer type III cells were observed as the incubation at the nonpermissive temperature continued. After incubation at 37°C for 4 h, only 6.4% of cells displayed such morphology. Furthermore, in the mutant cells arrested at high temperature, the length of cytoplasmic microtubules was longer and exhibited brighter fluorescent staining (Fig. 7, *C* and *E*) than those seen in the

Table II. cmd1-101 Mutant Increases Chromosome Loss

Culture condition	Frequency of chromosome loss (event/10^4 cells)	
	Wild-type	*cmd1-101* mutant
23°C 4 h	1.3	68.9
30°C 4 h	1.9	108.6
23°C 3 h, 37°C 1 h	1.3	165.7

Frequencies of chromosome loss for cells that had been incubated in YPGS at 23, 30, or 37°C. The strains GHGC300 and GHW300 were first grown to early-exponential phase in the selective medium. These cells were then transferred to fresh YPGS medium and incubated for 4 h at 23°C or 30°C, or 3 h at 23°C and then 1 h at 37°C. Viability was determined by plating out a portion of the culture on YPGS plates. The remaining cells were collected from culture and plated on SGS plate containing 1 mg/ml 5-FOA to select cells lacking a *URA3* chromosome fragment as described (Shero et al., 1991). The frequency of chromosome loss equals the number of Ura^- cells divided by the number of viable cells.

wild type cells (Fig. 7 *A*) or mutant cells grown at the permissive temperature (Fig. 7 *B*), suggesting that the cytoplasmic microtubules are abnormally developed. Moreover, some of the microtubules appeared to be unassociated with the spindle plaque (Fig. 7 *D*). The apparent disruption of microtubule organization is consistent with gross defects in chromosome segregation.

The defects in microtubule organization and chromosome segregation seen in the *cmd1-101* (GHGC1501) cells were found to result from the formation of a monopolar spindle. Serial sections through the entire nucleus in each of 37 large budded cells arrested at high temperature were examined by electron microscopy. In 32 nuclei (87%), only a single SPB was observed. No other structure resembling to a spindle plaque with or without attached microtubules was found. We have also examined the serial sections through the whole cell of four of the cells containing a single SPB, and no SPB that detached from the nuclear envelope was observed. The distribution of large budded cells containing a single SPB in such a high frequency was never observed in wild-type cells (YPH501). In wild-type cells, as the SPB duplication occurs early in cell cycle, budded cells in exponentially growing cultures should contain two SPBs at various stages of mitosis (Byers and Goetsch, 1975, also see Fig. 9 *C*). We found that all the budded cells (n = 13) of the *cmd1-101* GHGC1501 strain grown at 23°C contained two SPBs per nucleus (Fig. 9, *D–F*), each acting as a pole of the mitotic spindle as that seen in the wild cell (Fig. 9 *C*).

According to the number of SPB and the position of SPB localized, we found that the morphology of cells observed under electron microscope still could be divided into three types (Fig. 9, *G–M*; Fig. 10). These three types of microtubule organizations are corresponding to those observed by immunofluorescence microscopy, respectively (Fig. 7, *C–E*; Fig. 8).

We found that both the cells of type I and type II contained

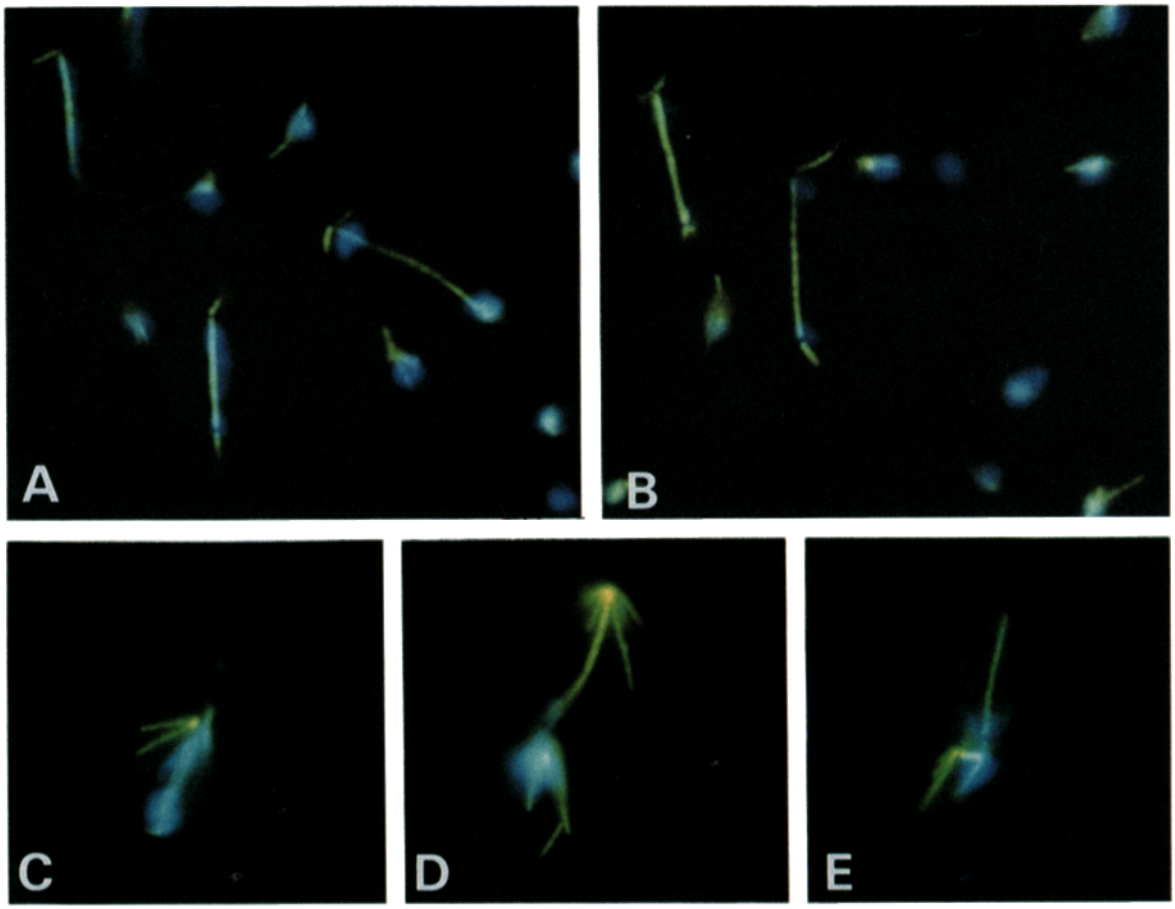

Figure 7. Immunofluorescent staining of wild-type and the *cmd1-101* mutant cells. Cells were stained to display microtubules with antitubulin antibody (FITC, *green*) and DNA with DAPI (*blue*). (*A*) Wild-type cells (YPH501); and (*B*) the *cmd1-101* mutant cell (GHGC1501) grown at 23°C in YPGS medium. *C*, *D*, and *E* show three typical types of microtubule organizations observed in the *cmd1-101* cells (GHGC1501) grown at 23°C to early exponential phase and transferred to 37°C for 3 h.

Time of incubation at 37°C (h)		Percentage of Cells Displaying (%) type I: The single SPB associated with the nuclear DNA	type II: The single SPB disassociated with nuclear DNA	type III: Short spindle
3	(n=540)	25.4	58.7	15.9
4	(n=670)	35.5	58.1	6.4

Figure 8. Cells from an exponential-phase culture of strain GHG-C1501 (*cmdl-101/cmdl-101*) grown in YPGS at 23°C were shifted to 37°C. At the indicated time point, samples were fixed and processed for antitubulin immunofluorescence and DAPI staining as described in Materials and Methods. The staining patterns of microtubules and nuclear DNA in the cells were examined and counted under a fluorescence microscope. Type I indicates morphology of a cell exhibiting a cluster of microtubules associated with the nuclear DNA; type II indicates a cell carrying a focus of microtubules unassociated with the nuclear DNA; type III shows a cell displaying a short spindle or spindle-like structure. "*n*" is the number of the total cells examined from three independent preparations of samples.

a single SPB. The SPB in type I cell appeared to attach to a deformed nucleus in the mother cells (see Fig. 9 *G*). Normally, the wild type SPB resides in the plane of the nuclear envelope with its inner and outer plaques on the nuclear and cytoplasmic faces, respectively (Fig. 9 *B*). However, type I SPBs were frequently embedded in an invagination of the nuclear envelope (Fig. 9, *G*, *H*). The location and orientation of the SPB appeared to be affected by irregular invaginations of the nuclear envelope. As shown in Fig. 9, *G–H* and Fig. 10 *A–D*, the flat plaques of the SPB appeared crossing the nuclear envelope vertically; half of its outer plaque was inside the interior of the nucleus so that the microtubules, which radiated from the same outer plaque, extended towards both the cytoplasmic and the nuclear region. On the other hand, the SPB in type II cells was found to have migrated into the distal region of the bud, where it resided near the tip of a thin extension of the nuclear envelope (Fig. 9 *I–L*). One characteristic feature observed in type II cells is that the single SPB did not localize exactly on the tip of the projection (Fig. 9, *I* and *J*). Instead, a bundle of nuclear microtubules protruded the nuclear envelope directly (Fig. 9 *K*, *L*, *M*). These nuclear microtubules may be responsible for the elongation of the nucleus and the movement of the projection of nuclear envelope into the bud. Moreover, these nuclear microtubules appeared to be unassociated with any spindle plaque like structure and ended with a caplike structure (Fig. 9, *L*, and *M*, *arrowhead*). It has previously been reported that the microtubule end proximal to the site of initiation on the SPB is distinguished as a "closed" end, which is only detected by negative-stained preparation of isolated SPB (Byers et al., 1978). Because we have not found this kind of detachment in wild-type cells by using the freeze-substituted fixation method, we presume that these microtubules might result from a poor association with some unknown components anchoring the microtubules on the plaques of SPB. Alternatively, it is also possible that these components may have been detached from the SPB to form these free ended microtubules (Fig. 9, *K–M*, *double arrows*). There are 13% of the cells (5/37) containing two SPBs (type III) 4 h after incubation at 37°C. Fig. 10 (*E* and *F*) show the typical morphology observed in the type III cells. The direction of the spindle was distorted from the long axis of nuclear elongation in all the five cells examined. Cells displaying type III morphologies were minor in cell specimens prepared after incubation for 4 h at 37°C. This result is consistent with the fluorescence microscopic observation. Majority of cells were arrested with a single SPB that formed a monopolar spindle (Fig. 8). These observations suggest that the spindle organization is inhibited in the *cmdl-101* mutant.

The multi-plaque structure of the single SPB in the three types appeared normal. The SPB was not enlarged as those observed in *cdc31* (Byers, 1981*b*) and *kar1* mutants (Rose and Fink, 1987), and did not contain an enlarged half bridge or an abnormal SPB without attached microtubules as those observed in *mps1* and *mps2* mutants (Winey et al., 1991). However, the perturbed association of microtubules with the spindle plaque and the altered location of the SPB on the nuclear envelope suggest that the function of SPB is affected in the *cmdl-101* mutant.

The Integrity of the Nucleus Is Apparently Disturbed in cmdl-101 Mutant

The morphology of the nucleus in *cmdl-101* cells appeared abnormal. When observed by the freeze-substituted fixation method, the morphology of the nucleus in wild-type cells always appears round and the nuclear contour is smooth (Fig. 9 *A*; also see Kanbe and Tanaka, 1989; Baba and Osumi, 1987, Baba et al., 1989). However, we found that the nuclear envelopes of the mutant cell formed invaginations even when the cells were incubated at the permissive temperature, although the morphology and duplication of SPB still appeared normal (Fig. 11, *A* and *B*) The deformation of the nucleus became more severe 2 h after shift to 37°C (Fig. 11, *C* and *D*). As the incubation at the nonpermissive temperature con-

Figure 9. Electron micrographs of the *cmdl-101* mutants. A normal spindle with normal SPBs are seen in *cmdl-101* cells (strain GHGC1501) grown at 23°C (*D*, *E*, and *F*) as well as that observed in wild-type cells (strain YPH501) (*A*, *B*, and *C*). The structure of SPB and microtubules observed using the freeze substituted fixation is well preserved and morphologically similar to that seen by the conventional method as described in Byers and Goestch (1975). After shift to 37°C for 4 h, the same strain displays two types of microtubule organizations which all produce monopolar spindle ((*G–M*) in serial sections. In type I cells, the SPB (*arrow*) lies at an invagination of the nuclear envelope, the microtubules initiated from the outer plaque extend toward both the cytoplasmic and nuclear interiors (*G*). *H* is the magnification of the region around the SPB in *G*. In type II, the SPB (*arrows* indicate the position of the SPB) located at the projection (boxed in *I*) of the nuclear envelope (*I*, *J*). *J*, *K*, and *L* are three adjacent sections. The nuclear microtubules ended with a caplike structure (*L* and *M*, *arrowhead*) and protruded the nuclear envelope directly. *N*, nucleus; *V*, vacuole; *mt*, microtubule.

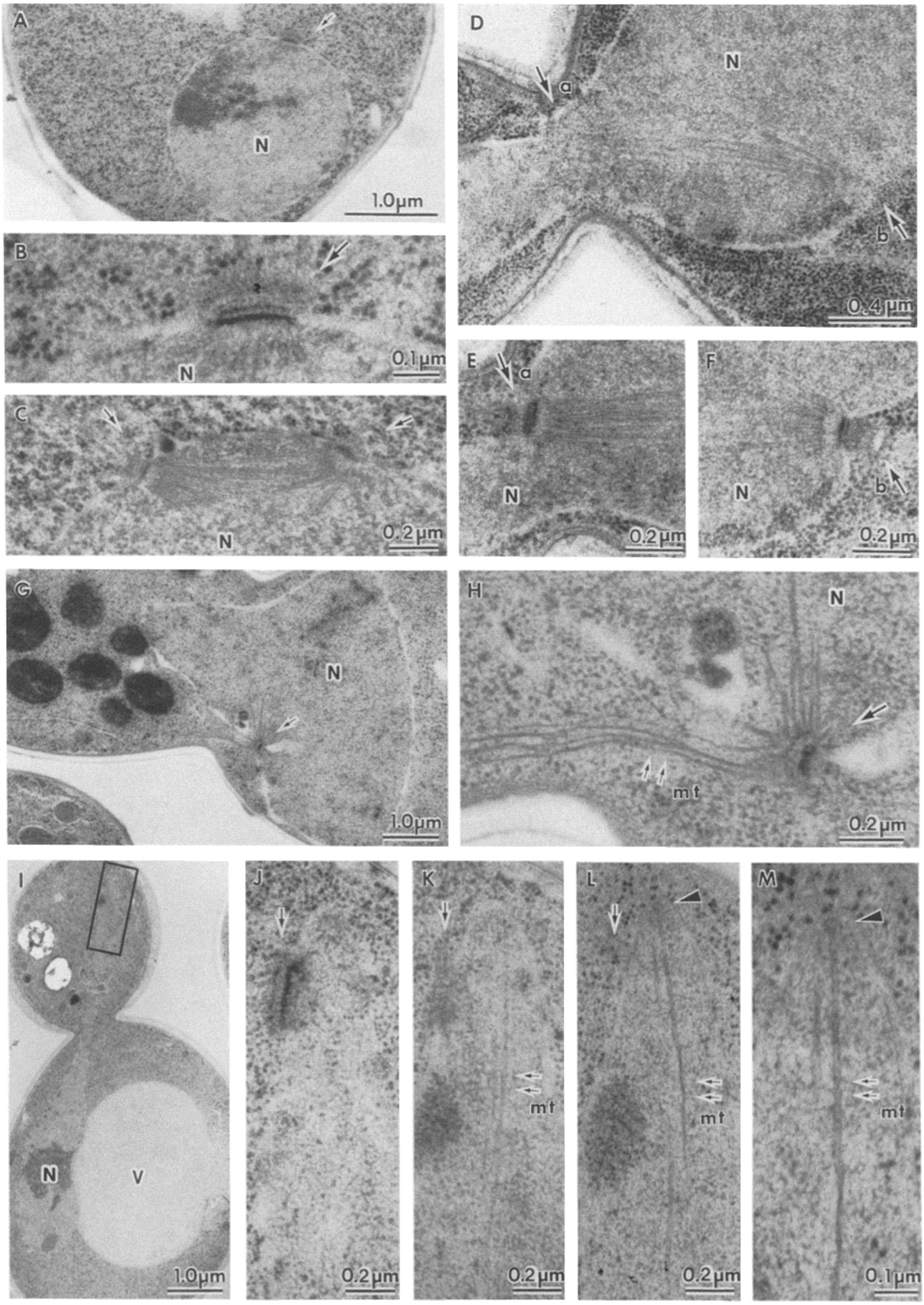
A
N
1.0μm
B
N
0.1μm
C
N
0.2μm
D
N
a
b
0.4μm
E
a
N
0.2μm
F
N
b
0.2μm
G
N
1.0μm
H
N
mt
0.2μm
I
N
V
1.0μm
J
0.2μm
K
mt
0.2μm
L
mt
0.2μm
M
mt
0.1μm

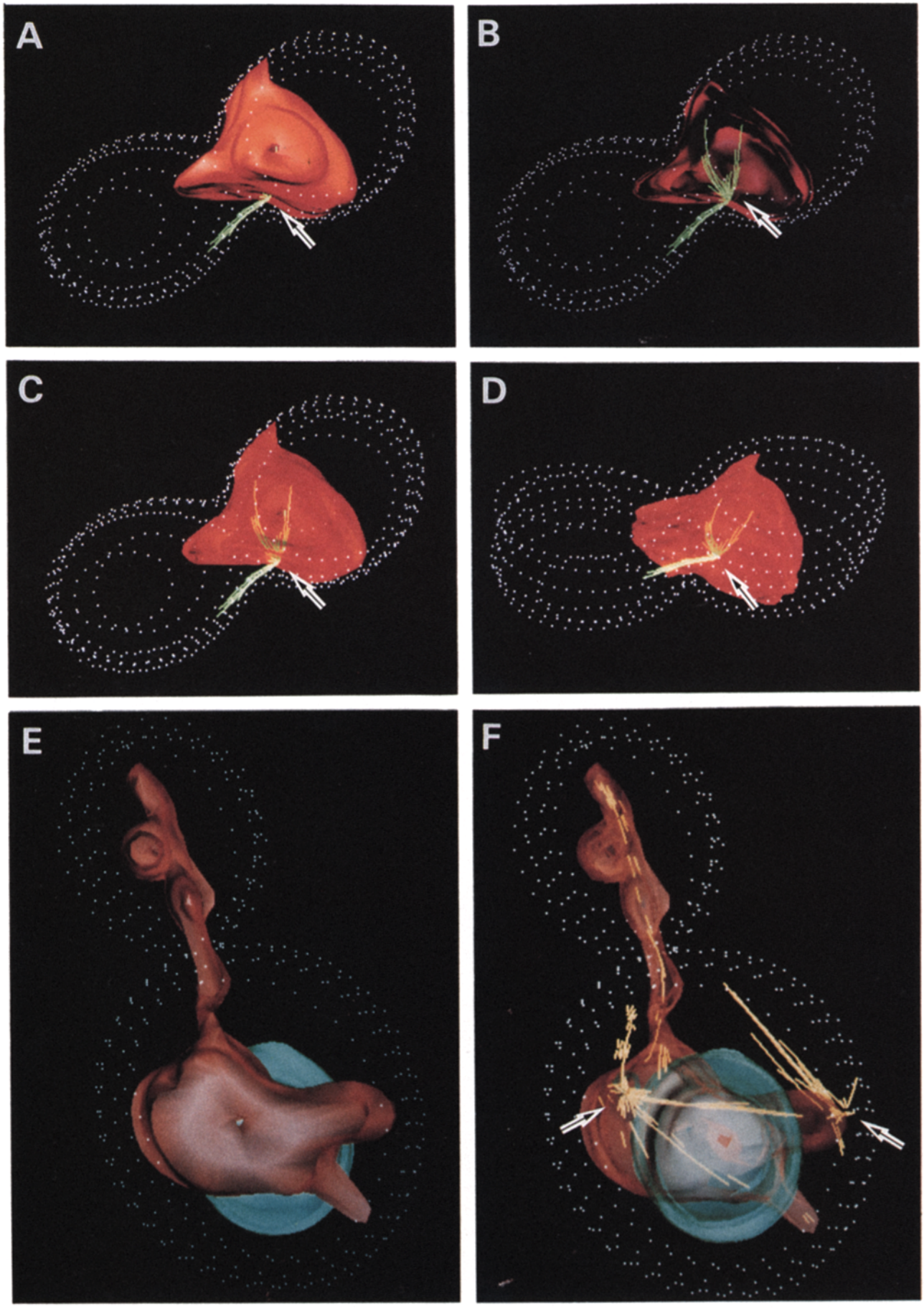
A
B
C
D
E
F

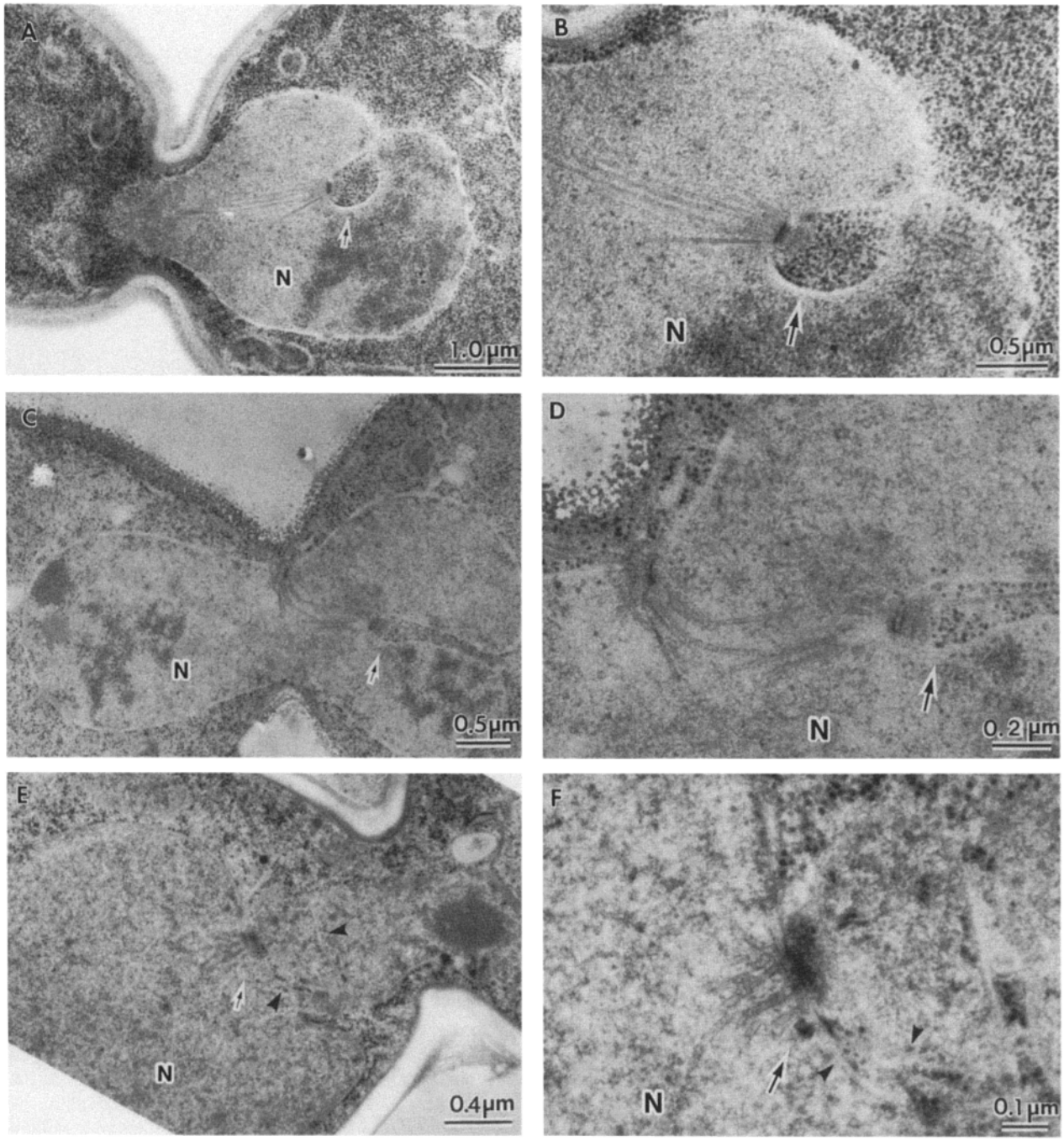

Figure 11. The morphology of nucleus in the *cmdl-101* mutant. The nuclear envelope observed in *cmdl-101* cells (GHGC1501) incubated at 23°C (*A* and *B*) forms invaginations using the freeze-substituted fixation method. The nuclear envelope deforms more severe after incubation at 37°C for 2 h (*C* and *D*). As the incubation at 37°C continues (5.5 h), the nuclear envelope becomes more intricate and the fragmentation of the nucleus begins (*E* and *F*). Arrows indicate the invagination of nuclear envelope; arrowheads indicate the nuclear envelope. *N*, nucleus.

Figure 10. Three-dimensional reconstruction from serial thin sections. (*A–D*) The three dimensional image of the type I cell shown in Fig. 9, *G* and *H*. (*E–F*) The three-dimensional image of the type III cell. The plasma membranes are represented by dotted lines (*white*), the nuclear envelope was represented by a nontransparent surface (*red*, *A*, *B*, and *E*) or semitransparent surface (*C*, *D*, and *F*). The microtubules appear as solid lines (*green* in *A–D* and *yellow* in *E–F*). The vacuole is represented by a nontransparent (*E*) or transparent surface (*F*, *blue*). *A*, *C*, *E*, and *F* are top views of the cell, *D* is a view from the side. *B* is the top view of the section phase where the SPB located. Arrows indicate the positions of the SPB.

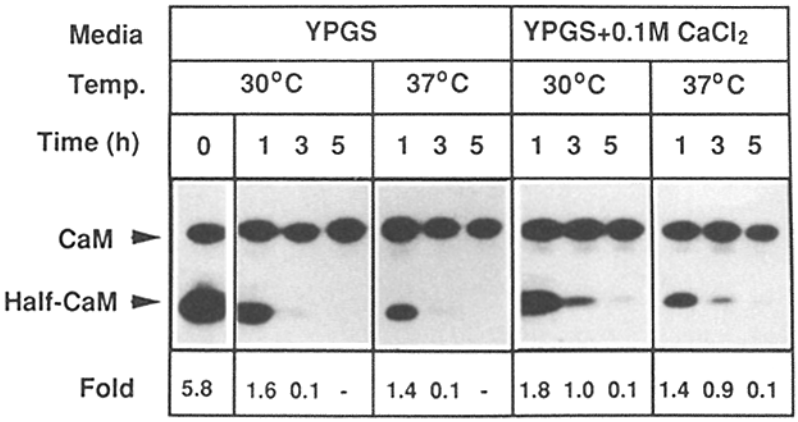

Figure 12. Pulse-chase experiment of the carboxyl-terminal half CaM with antibody against yeast CaM. Diploid strain GHGC1502 (*cmdl-101/CMD1*) which expresses both the carboxyl-terminal half CaM and the native CaM was used. The pulse and chase were performed as described in Materials and Methods. The immunoprecipitates were resolved by 15% sodium dodecyl sulfate polyacrylamide gel electrophoresis. After electrophoresis, the gel was dried and exposed to film overnight. The file was then scanned with a densitometer. The "fold" is the rate of expression level of the half CaM over that of the wild-type CaM (mol/mol) at each indicated time point.

tinued, the nuclear envelope formed irregular projections and invaginations (also see Fig. 10, *E* and *F*). Upon incubation for 5.5 h at 37°C, the nucleus became fragmented and the nuclear envelope appeared very intricate as shown in Fig. 11, *E* and *F*.

Pulse-Chase Experiment

The half CaM mutant showed a temperature-sensitive phenotype. The temperature-sensitive growth was partially rescued in a Ca^{2+}-rich medium (Sun et al., 1991). We have examined the stability of the half CaM at 30°C and 37°C using a diploid strain GHGC1502. One copy of the chromosomal *CMD1* genes of strain GHGC1502 was replaced with the *GALlp-cmdl-101* fusion gene. Thus, this diploid strain expresses both the half CaM and the native CaM when grown in the galactose medium, and does not show a Ts^- phenotype. Using this strain we could examine the stability of the half CaM without considering the effect resulting from the loss of viability of cells at the nonpermissive temperature. As shown in Fig. 12, the native CaM appeared stable at both temperatures, whereas the stability of the half CaM was apparently lower than that of the native protein. The low stability may be one of the reasons why the functional complementation of the half CaM is only observed when it is expressed under the control of a strong promoter (Sun et al., 1991).

Discussion

We have described the characterization of the recessive chromosomal *cmdl-101* mutation, which expresses a truncated yeast CaM consisting of only the carboxyl-terminal half domain (Met ^{72}-Cys^{147}). Cells depending solely on the half CaM show a temperature sensitive and Ca^{2+}-remedial phenotype for growth.

The terminal phenotype of the *cmdl-101* mutant is quite uniform: a large bud and a G2/M DNA content (Figs. 4 *B* and 5). These phenotypes indicate that the *cmdl-101* mutation causes defects at the G2/M phase of the cell cycle. Unlike all previously described *cdc* mutants (Johnston et al., 1977; Pringle and Hartwell, 1981), this conditional CaM mutant contains two unique features: the first is the large deletion mutation within the structure of the CaM (half CaM), and the second is that the mutant CaM is designed to be expressed under the control of a strong promoter. The half CaM expressed under the authentic *CMD1* promoter does not complement the *cmdl* null mutation (Sun et al., 1991). Thus, this mutant allele can not be isolated like a typical *cdc* mutation.

Several lines of evidence indicate that the *cmdl-101* mutation inhibits the normal functions of SPB and mitotic spindle. Genetic studies show that the *cmdl-101* temperature sensitive mutation increases the frequency of chromosome loss, a phenotype resulting from defects in chromosome segregation (Table II). Immunofluorescence analysis of the mutant cells arrested at high temperature strongly suggests that the SPB fails to form a normal mitotic spindle (Fig. 7, *C* and *D*; see also Fig. 8). Electron microscopic analyses of serial sections of arrested mitotic cells show directly that, in these cells, only a single SPB is observed and the location of the SPB on the nuclear envelope is abnormal. Furthermore, the association of nuclear microtubules with the SPB is also affected (Fig. 9, *K–L*). In addition, we have also examined the phenotype of cells depleted of the half CaM: electron microscopy revealed that all the cells ($n = 5$) depleted of the half CaM had a single SPB and formed monopolar spindle (Sun, G.-H., A. Hirata, Y. Ohya, and Y. Anraku, unpublished data). Taken together, these results suggest an essential role of CaM in spindle organization and SPB functions.

A number of mutations in yeast, for instance, *cdc31* (Baum et al., 1986), *ndc1* (Thomas and Botstein, 1986), *kar1* (Rose and Fink, 1987), *esp1* (Baum et al., 1988), *mps1* and *mps2* (Winey et al., 1992) have been reported to cause defects in the duplication and functions of SPB. The *cmdl-101* mutant shares many characteristic phenotypes with the *cdc31*, *kar1*, and *mps1* mutants including formation of a monopolar spindle, abnormal localization of SPB in the invagination of the nuclear envelope. There are still some distinct phenotypes: the morphology or the size of the SPB appears to be affected in these three mutants, while these features of the SPB in the *cmdl-101* appear normal. In addition, the orientation of the SPB on the nuclear envelope and the association of microtubules with the SPB are notably interfered in the *cmdl-101* mutant. Among these previously reported reported genes, the *CDC31* gene which is required for SPB duplication has been found to encode a Ca^{2+}-binding protein similar to CaM (Baum et al., 1986). We found that overexpression of the half CaM in the *cdc31* mutant, or combination of the *cmdl-101* with the *cdc31* mutations showed no synthetic phenotype (G.-H. Sun, Y. Ohya, and Y. Anraku, unpublished data).

We have shown that the *cmdl-101* mutation caused defects

in SPB functions and formed abnormal monopolar spindles at the nonpermissive temperature. How do these monopolar spindles arise? Which step(s) in the process of spindle organization require CaM functions? There are several considerable possibilities. First, it is possible that the CaM function is required for SPB duplication. The failure in SPB duplication results in a high percentage of cells containing a single SPB which forms monopolar spindle. We found that the size of the single SPB in the *cmdl-101* cells was not significantly enlarged, and the morphology was similar to that of SPB in G_0 phase of the cell cycle. These observations suggest that execution of the CaM functions is at an early step in the pathway of SPB duplication. It is also possible that CaM has more than one execution point during the formation of mitotic spindle. Indeed, there are ~10% of cells exhibiting bipolar short spindle (type III). These cells are probably the population that has escaped the critical point(s) at the early step of SPB duplication that requires the CaM function. We found that the organizations of the short spindle in these cells are abnormal: (*a*) one of the two SPBs was frequently embedded in the deep invagination of the nuclear envelope (Fig. 11, *C* and *D*), and (*b*) the orientation of the short spindle was always different from the direction of nuclear elongation (Fig. 10, *E* and *F*). These abnormal organizations suggest that functions of the SPB in the bipolar spindle are also affected by the *cmdl-101* mutation. Finally, we have found that the cell number did not increase after incubation for 3 h at 37°C (Fig. 5). However, the type III cells were falling, whereas the type I cells with the monopolar spindle were increasing (Fig. 8). These observations may indicate that some cells with bipolar spindle have converted into cells exhibiting monopolar spindle without cell division. This result suggests that CaM may be also required for the integrity and stability of SPB. It is possible that the SPB duplication in type III cells is interfered by a loss of CaM function. Thus, a defective SPB is formed and then broken down at the nonpermissive temperature. It is experimentally difficult to follow and examine the morphological changes of the same SPB at different time points. It must be informative to examine the morphology of SPB using a synchronized culture, or the synthetic phenotypes of the *cmdl-101* with the other mutations causing defects in SPB duplication.

The carboxyl-terminal and the amino-terminal halves of CaM show very high homology to each other. Each of the half domains forms a lobe of the dumbbell structure of the entire CaM molecule (Babu et al., 1985, 1988). Functional complementation of the *cmdl* null mutation with both the half molecules suggests that the function of CaM involved in SPB functions and organization of microtubules might depend only on one of its two structurally similar domain, not its global structure. We have found that cells expressing only the amino-terminal half CaM show a similar phenotype with that observed in cells expressing the carboxyl-terminal half (Sun, G.-H., Y. Ohya, and Y. Anraku, unpublished data). It is possible that the half CaM regulates the process of PBS duplication and spindle formation through activation of CaM-dependent enzymes. It is also possible that each of the half domains might perform as a temporal component of the spindle or SPB structure.

The cytoplasmic microtubules also appear abnormally developed in the *cmdl-101* mutant incubated at the nonpermissive temperature. The abnormal development and organization of cytoplasmic microtubules are consistent with previous studies that have shown that CaM has a protective effect on microtubules. Microinjection of CaM into PtK_1 cells has a stabilizing effect on kinetochore microtubules (Sweet et al., 1988). The 145-K STOP protein, a CaM-binding protein described by Margolis and co-workers (1986) confers cold-stability to brain microtubules (Pabion et al., 1984). We have found that combination of the *cmdl-101* mutation with *tub2-150* mutation (Stearns et al., 1990), which stabilizes microtubules and requires benomyl for mitotic growth at high temperature, caused more strict Ts^- growth than with other tubulin mutation alleles (G.-H. Sun, Y. Ohya, and Y. Anraku, unpublished data). This result is consistent with the aberrant organization of cytoplasmic microtubules seen in the *cmdl-101* cells, suggesting that the mutant CaM may have an effect causing an excessive stabilization or incorrect assembly of microtubules.

Immunofluorescent staining studies have shown that CaM localizes to the centriolar region and to the kinetochore-to-pole microtubules in various cells (Welsh et al., 1978, 1979). Fluorescent CaM, microinjected into cells, appears at the same sites (Zavortnik et al., 1983). This concentrated localization of CaM in the mitotic apparatus suggests an important role for CaM in the corresponding process. The formation of monopolar spindle observed in the *cmdl-101* mutant allele is consistent with the distribution of CaM observed in higher organisms. In *S. cerevisiae*, it is still not clear whether the yeast CaM is a component of SPB or temporally associated with the mitotic apparatus. The immunofluorescence staining with antibody against yeast CaM reveals that CaM is present throughout the cytoplasm at all stages of the cell cycle and is concentrated in the site of bud growth (Sun et al., 1992). The immunolocalization of the half CaM in the *cmdl-101* cells grown at permissive temperature is similar to that of native CaM observed in wild-type cells (data not shown). It may be possible that the concentration of CaM required for SPB and spindle functions is lower than that for bud growth. The immunofluorescence microscopy alone cannot specify a precise localization of yeast CaM in the mitotic apparatus. It must be informative to examine the localization of yeast CaM in the mitotic apparatus using immunoelectron microscopy.

The mitotic arrest phenotypes, including specific arrest at G2/M phase and an elevated rate of chromosome loss observed in the *cmdl-101* mutant, are consistent with the phenotypes observed in a CaM depleted mutant (Ohya and Anraku, 1989*a*). As CaM is a stable protein and requires 12–15 h (approximately six generations) to remove the protein completely, we found that the terminal phenotype of the CaM depleted mutant is not as uniform as that caused by the *cmdl-101* temperature sensitive mutation. The percentage of cells arrested with small bud is higher in the CaM depleted cells than in the *cmdl-101* cells. It is possible that other processes (e.g., bud growth) which require CaM functions are also affected in the CaM depleted mutant.

Using the freeze-substituted fixation method, combined with a sufficient number of serial sections of better preserved nuclei, we were able to dissect the nuclear morphology in the *cmdl-101* mutant (Fig. 11). We found that the integrity of the nuclear envelope in the *cmdl-101* mutant cells at nonpermissive temperature was significantly perturbed (Figs. 10 and 11). One possibility is that the alteration in normal SPB

and spindle function may develop abnormal morphologies of the nuclear envelope. Similar phenotype has also been observed with the *kar1* mutation, which causes a defect in SPB duplication (Rose and Fink, 1987). It may also be possible that CaM is simultaneously required for maintenance of nuclear envelope integrity. We found that the *cmd1-101* mutant loses the viability rapidly upon shift to nonpermissive temperature. This phenotype is different from the *cdc31* and *mps2* mutants that also form monopolar spindle at the nonpermissive temperature. These two mutants exhibit good viability at the transient arrest and increase the ploidy upon the return to permissive conditions (Schild et al., 1981, Winey et al., 1991). We presume that the perturbed integrity of the nuclear envelope may also affect the viability of the *cmd1-101* cells at high temperature.

The pulse chase experiment showed that the stability of the half CaM at the nonpermissive temperature (37°C) was not very different from that at 30°C, a temperature at which the *cmd1-101* cells still grow well (see Fig. 2). One possibility for the Ts^- growth phenotype is that a very little decrease causes a severe defect. If this is true, an increase in the expression level of the mutant CaM should rescue the temperature sensitive phenotype. To verify this possibility, we have transformed the *cmd1-101* strain with plasmid pRSGCAMC1 which is a high copy plasmid carrying the *GALp-cmd1-101* fusion gene. Even though the expression level of the half CaM was elevated, the cells still exhibited a temperature sensitive phenotype similar to those without the expression plasmid (data not shown). These results suggest that the instability of the mutant protein may not be the primary cause of the temperature sensitive phenotype. We presume that the high temperature may block the functional interaction of CaM with its target proteins. The high concentration of extracellular Ca^{2+} ion partially rescued the Ts^- growth of the *cmd1-101* cells, but did not show any effect on the growth of the cells depleted of the half CaM (data not shown). The degradation of the half CaM was still faster than that of the native protein when cells were grown in medium containing $CaCl_2$ supplement. These results suggest that the addition of Ca^{2+} ion may activate the interaction of the mutant CaM with its targets (Anraku et al., 1991). Future investigations on the crucial targets of CaM will determine the molecular mechanisms of CaM involved in spindle organization and SPB functions.

We are grateful to Dr. Teruhiko Beppu, Dr. Minoru Yoshida and Dr. Takeo Usui for their kind instruction and technical help on flow cytometric analysis, to Dr. David Botstein for the *tub* mutants, and to Dr. Tsuneyoshi Kuroiwa for his detailed instruction and help in carrying out the three-dimensional reconstruction and VIMPCS measurement. We thank Dr. Mark Rose for general discussions and criticism, Dr. Rebecca Bernat, Dr. Akihiko Nakano, and Dr. Yoh Wada for critical reading of the manuscript.

This work was supported in part by Grant-in-Aid 0325612 (Y. Ohya) for Scientific Research on Priority Areas from the Ministry of Education, Science, and Culture of Japan, and a grant from the Japan Society for the Promotion of Science for Japanese Junior Scientists to G.-H. Sun.

Received for publication 9 July 1992 and in revised form 9 September 1992.

References

Anraku, Y., Y. Ohya, and H. Iida. 1991. Cell cycle control by calcium and calmodulin in *Saccharomyces cerevisiae*. *Biochim. Biophys. Acta.* 1093: 169–177.

Baba, M., and M. Osumi. 1987. Transmission and scanning electron microscopic examination of intracellular organelles in freeze-substituted *Klockera* and *Saccharomyces cerevisiae* yeast cells. *J. Electr. Microsci.* 5:249–261.

Baba, M., N. Baba, Y. Ohsumi, K. Kanaya, and M. Osumi. 1989. Three-dimensional analysis of morphogenesis induced by mating pheromone a factor in *Saccharomyces cerevisiae*. *J. Cell Sci.* 94:207–216.

Babu, Y. S., J. S. Sack, T. J. Greenhough, C. E. Bugg, A. R. Means, and W. J. Cook. 1985. Three-dimensional structure of calmodulin. *Nature (Lond.).* 315:37–40.

Babu, Y. S., C. E. Bugg, and W. J. Cook. 1988. Structure of calmodulin at 2.2 Å resolution. *J. Mol. Biol.* 204:191–204.

Baum, P., C. Furlong, and B. Byers. 1986. Yeast gene required for spindle pole body duplication: homology of its product with Ca^{2+}-binding proteins. *Proc. Natl. Acad. Sci. USA.* 83:5512–5516.

Baum, P., C. Yip, L. Goetsch, and B. Byers. 1988. A yeast gene essential for regulation of spindle pole duplication. *Mol. Cell Biol.* 8:5386–5397.

Boeke, J. D., J. Trueheart, G. Natsoulis, and G. R. Fink. 1987. 5-fluoro-orotic acid as a selective agent in yeast molecular genetics. *Methods Enzymol.* 154:164–175.

Brady, R. C., F. Cabral, and J. R. Dedman. 1986. Identification of a 52-kD calmodulin-binding protein associated with the mitotic spindle apparatus in mammalian cells. *J. Cell Biol.* 103:1855–1861.

Byers, B., and L. Goetsch. 1975. Behaviour of spindles and spindle plaques in the cell cycle and conjugation in *Saccharomyces cerevisiae*. *J. Bacteriol.* 124:511–523.

Byers, B., K. Shriver, and L. Goetsch. 1978. The role of spindle pole bodies and modified microtubule ends in the initiation of microtubule assembly in *Saccharomyces cerevisiae*. *J. Cell Sci.* 30:331–352.

Byers, B. 1981*a*. Cytology of the yeast life cycle. *In* The Molecular Biology of the Yeast *Saccharomyces cerevisiae*. J. N. Strathern, E. W. Jones, and J. R. Broach, editors. Cold Spring Harbor Laboratory, Cold Spring Harbor, New York. 59–96.

Byers, B. 1981*b*. Multiple roles of the spindle pole bodies in the life cycle of *Saccharomyces cerevisiae*. *In* Molecular Genetics in Yeast. D. V. Wettstein, A. Stenderup, M. Kielland-Brandt, and J. Friis, editor. Munksgaard International Publishers, Ltd., Copenhagen. 119–131.

Carle, G., and M. Olson. 1984. Separation of chromosomal DNA molecules from yeast by orthogonal-field-alteration gel electrophoresis. *Nucleic Acids Res.* 12:5647–5664.

Carle, G., and M. Olson. 1985. An electrophoretic karyotype for yeast. *Proc. Natl. Acad. Sci. USA.* 82:3756–3760.

Cohen, P., and C. B. Klee. 1988. Calmodulin, Vol. 5: Molecular Aspects of Cellular Regulation. P. Cohen and C. B. Klee, editors. Elsevier Science Publishers B. V., Amsterdam, The Netherlands.

Daniel, B., R. Bartlett, K. Crawford, and P. Nurse. 1991. Involvement of p34cdc2 in establishing the dependency of S phase on mitosis. *Nature (Lond.).* 349:388–393.

Davis, T. N., and J. Thorner. 1989. Vertebrate and yeast calmodulin, despite significant sequence divergence, are functionally interchangeable. *Proc. Natl. Acad. Sci. USA.* 86:7909–7913.

Davis, T. N., M. S. Urdea, F. R. Masiarz, and J. Thorner. 1986. Isolation of the yeast calmodulin gene: calmodulin is an essential protein. *Cell.* 47: 423–431.

Hartwell, L. H. 1971. Genetic control of the cell division cycle in yeast II. Genes controlling DNA replication and its initiation. *J. Mol. Biol.* 59: 183–194.

Hartwell, L. H. 1978. Cell division from a genetic perspective. *J. Cell Biol.* 77:627–637.

Hutter, K.-J., and H. E. Eipel. 1979. Microbial determination by flow cytometry. *J. Gen Microbiol.* 132:979–988.

Ito, H., Y. Fukuda, K. Murata, and A. Kimura. 1983. Transformation of intact yeast cells treated with alkali cations. *J. Bacteriol.* 153:163–168.

Johnston, G. C., J. R. Pringle, and L. H. Hartwell. 1977. Coordination of growth with cell division in the yeast *Saccharomyces cerevisiae*. *Mol. Cell Biol.* 4:1440–1448.

Johnston, M., and R. W. Davis. 1984. Sequences that regulate the divergent GAL1-GAL10 promoter in *Saccharomyces cerevisiae*. *Mol. Cell Biol.* 4:1440–1448.

Kanbe, T., and K. Tanaka. 1989. Dynamics of cytoplasmic organelles in the cell cycle of the fission yeast Schizosaccharomyces pombe: three-dimensional reconstruction from serial sections. *J. Cell Sci.* 94:647–656.

Kilmartin, J., B. Wright, and C. Milstein. 1982. Rat monoclonal antitubulin antibodies derived by using a new nonsecreting rat cell line. *J. Cell Biol.* 93:576–582.

Kuroiwa, T., S. Miyamura, S. Kawano, M. Hizume, A. Toh-e, I. Miyakawa, and N. Sando. 1986. Cytological characterization of NOR in the bivalent of *Saccharomyces cerevisiae*. *Exp. Cell Res.* 165:199–206.

Laemmli, U. K. 1970. Cleavage of structural proteins during the assembly of the head of bacteriophage T4. *Nature (Lond.).* 227:680–685.

Maniatis, T., E. F. Fritsch, and J. Sambrook. 1982. Molecular Cloning: A Laboratory Manual. Cold Spring Harbor Laboratory, Cold Spring Harbor, New York.

Margolis, R. L., C. T. Rausch, and D. Job. 1986. Purification and assay of a 145-kDa protein (STOP145) with microtubule-stabilizing and motility behavior. *Proc. Natl. Acad. Sci. USA.* 83:639–643.

Nisogi, H., K. Kominami, K. Tanaka, A. Toh-e. 1992. A new essential gene of *Saccharomyces cerevisiae* a defect in it may result in instability of nucleus. *Exp. Cell Res.* 200:48–57.

Ohya, Y., and Y. Anraku. 1989*a*. A galactose-dependent *cmd1* mutant of *Saccharomyces cerevisiae*: involvement of calmodulin in nuclear division. *Curr. Genet.* 15:113–120.

Ohya, Y., and Y. Anraku. 1989*b*. Functional expression of chicken calmodulin in yeast. *Biochem. Biophys. Res. Commun.* 158:541–547.

Ohya, Y., I. Uno, T. Ishikawa, and Y. Anraku. 1987. Purification and biochemical properties of calmodulin from *Saccharomyces cerevisiae*. *Eur. J. Biochem.* 168:13–19.

Ohya, Y., H. Kawasaki, K. Suzuki, J. Londesborough, and Y. Anraku. 1991. Two yeast gene encoding calmodulin-dependent protein kinases: isolation, sequencing, and bacterial expressions of *CMK1* and *CMK2*. *J. Biol. Chem.* 266:12784–12794.

Pabion, M., D. Job, and J. Margolis. 1984. Sliding of STOP proteins on microtubules. *Biochemistry.* 23:6642–6646.

Pringle, J. R., and L. H. Hartwell. 1981. The *Saccharomyces cerevisiae* cell cycle. *In* Molecular Biology of the Yeast *Saccharomyces*: Life Cycle and Inheritance. J. N. Strathern, E. W. Jones, and J. R. Broach, editors. Cold Spring Harbor Laboratory, Cold Spring Harbor, New York. pp. 97–142.

Rasmussen, C. D., and A. R. Means. 1987. Calmodulin is involved in regulation of cell proliferation. *EMBO (Eur. Mol. Biol. Organ.) J.* 6:3961–3968.

Rasmussen, C. D., and A. R. Means. 1989. Calmodulin is required for cell-cycle progression during G1 and mitosis. *EMBO (Eur. Mol. Biol. Organ.) J.* 8:73–82.

Rasmussen, C. D., R. L. Means, K. P. Lu, G. S. May, and A. R. Means. 1990. Characterization and expression of the unique calmodulin gene of *Aspergillus nidulans*. *J. Biol. Chem.* 265:13767–13775.

Rose, M. D., and G. R. Fink. 1987. *KAR1*, a gene required for function of both intracellular and extranuclear microtubules in yeast cell. *Cell.* 48:1047–1060.

Rose, M. D., F. Winston, and P. Hieter. 1990. Methods in Yeast Genetics. Cold Spring Harbor Laboratory, Cold Spring Harbor, New York.

Rothstein, R. 1983. One-step gene disruption in yeast. *Methods. Enzymol.* 101:202–211.

Schild, D., H. N. Ananthaswamy, and R. K. Mortimer. 1981. An endomitotic effect of a cell cycle mutation of *Saccharomyces cerevisiae*. *Genetics.* 97: 551–562.

Shero, J. H., M. Koval, F. Spencer, R. E. Palmer, P. Hieter, and D. Koshland. 1991. Analysis of chromosome segregation in *Saccharomyces cerevisiae*. *Methods Enzymol.* 194:749–765.

Sikorski, R. S., and P. Hieter. 1989. A system of shuttle vectors and yeast host strains designed for efficient manipulation of DNA in *Saccharomyces cerevisiae*. *Genetics.* 122:19–27.

Southern, E. M. 1975. Detection of specific sequences among DNA fragments separated by gel electrophoresis. *J. Mol. Biol.* 98:503–517.

Stearns, T., and D. Botstein. 1988. Unliked noncomplementation: isolation of new conditional-lethal mutations in each of the tubulin genes of *Saccharomyces cerevisiae*. *Genetics.* 119:249–260.

Stearns, T., M. A. Hoyt, and D. Botstein. 1990. Yeast mutants sensitive to antimicrotubule drugs define three genes that affect microtubule function. *Genetics.* 124:251–262.

Sun, G.-H., Y. Ohya, and Y. Anraku. 1991. Half-calmodulin is sufficient for cell proliferation: expressions of N and C-terminal halves of calmodulin in the yeast *Saccharomyces cerevisiae*. *J. Biol. Chem.* 266:7008–7015.

Sun, G.-H., Y. Ohya, and Y. Anraku. 1992. Yeast calmodulin localized to sites of cell growth. *Protoplasma.* 166:110–113.

Sweet, S. C., C. M. Rogers, and M. J. Welsh. 1988. Calmodulin stabilization of kinetochore microtubule structure to the effect of nocodazole. *J. Cell Biol.* 107:2243–2251.

Takeda, T., and M. Yamamoto. 1987. Analysis and in vivo disruption of the gene coding for calmodulin in *Schizosaccharomyces pombe*. *Proc. Natl. Acad. Sci. USA.* 84:3580–3584.

Thomas, J. H., and D. Botstein. 1986. A gene required for the separation of chromosomes on the spindle apparatus in yeast. *Cell.* 44:65–76.

Vollrath, D., R. W. Davis, C. Connelly, and P. Hieter. 1988. Physical mapping of large DNA by chromosome fragmentation. *Proc. Natl. Acad. Sci. USA.* 85:6027–6031.

Welsh, M. J., J. R. Dedman, B. R. Brinkley, and A. R. Means. 1978. Calcium-dependent regulatory protein: localization in mitotic apparatus of eukaryotic cells. *Proc. Natl. Acad. Sci. USA.* 75:1867–1871.

Welsh, M. J., J. R. Dedman, B. R. Brinkley, and A. R. Means. 1979. Tubulin and calmodulin. Effects of microtubules and microfilament inhibitors on localization in the mitotic apparatus. *J. Cell Biol.* 81:624–634.

Winey, M, and B. Byers. 1992. The spindle pole body of *Saccharomyces cerevisiae*: a model for genetic analysis of the centrosome cycle. *In* The Centrosome. V. Kalnins, editor Academic Press, Orlando, FL. 201–222.

Winey, M., L. Goetsch, P. Baum, and B. Byers. 1991. *MPS1* and *MPS2*: Novel yeast genes defining distinct steps of spindle pole body duplication. *J. Cell Biol.* 114:745–754.

Zavortnik, M., M. J. Welsh, and J. R. MacIntosh. 1983. The distribution of calmodulin in living mitotic cells. *Exp. Cell Res.* 149:375–385.